HSV Color Histogram and Directional Binary Wavelet Patterns for Content Based Image Retrieval

P.Vijaya Bhaskar Reddy[1]
[1]Research Scholar, Dept. of Computer Science & Engineering, SVU, Tirupati, A.P.
Dr.A.Rama Mohan Reddy[2]
[2]Head & Professor, Dept. of Computer Science & Engineering, SVU, Tirupati, A.P.
K.Guru Jyotsna Devi[3]
[3] Assistant Professor, CSE Dept., Priya Darsini Engineering College, Nellore
[1]bhskr.dwh@gmail.com , [2]ramamohansvu@yahoo.comP. [3]k.jyothsnadevi515@gmail.comV.

***Abstract*— This paper presents a new image indexing and retrieval algorithm by integrating color (HSV color histogram) and texture (directional binary wavelet patterns (DBWP)) features. For color feature, first the RGB image is converted to HSV image, and then histograms are constructed from HSV spaces. For texture feature, an 8-bit grayscale image is divided into eight binary bit-planes, and then binary wavelet transform (BWT) on each bitplane to extract the multi-resolution binary images. The local binary pattern (LBP) features are extracted from the resultant BWT sub-bands. Two experiments have been carried out for proving the worth of our algorithm. It is further mentioned that the database considered for experiments are Corel 1000 database (DB1), and MIT VisTex database (DB2). The results after being investigated show a significant improvement in terms of their evaluation measures as compared to HSV histogram and DBWP.**

Keywords- Directional Binary Wavelet Patterns (DBWP); Local Binary Patterns (LBP); Feature Extraction; HSV histogram; Image Retrieval.

I. INTRODUCTION

A. Motivation

Since the 1990s, content-based image retrieval (CBIR) has become an active and fast-advancing research area in image retrieval. In a typical CBIR, features related to visual content such as shape, color, and texture are first extracted from a query image, the similarity between the set of features of the query image and that of each target image in a DB is then computed, and target images are next retrieved which are most similar to the query image. Extraction of good features which compactly represent a query image is one of the important tasks in CBIR. Shape is a visual feature that describes the contours of objects in an image, which are usually extracted from segmenting the image into meaningful regions or objects. However, since it is difficult to achieve such image segmentation for natural images, the use of shape features in image retrieval has been limited to special applications where the extraction of object contours is readily available such as in trademark images. Comprehensive and extensive literature survey on CBIR is presented in [1]–[4].

Color is one of the most widely used visual features and is invariant to image size and orientation. Swain et al. proposed the concept of color histogram in 1991 and also introduced the histogram intersection distance metric to measure the distance between the histograms of images [5]. Stricker et al. used the first three central moments called mean, standard deviation and skewness of each color for image retrieval [6]. Pass et al. introduced color coherence vector (CCV) [7]. CCV partitions the each histogram bin into two types, i.e., coherent, if it belongs to a large uniformly colored region or incoherent, if it does not. Huang et al. used a new color feature called color correlogram [8] which characterizes not only the color distributions of pixels, but also spatial correlation of pair of colors. Lu et al. proposed color feature based on vector quantized (VQ) index histograms in the discrete cosine transform (DCT) domain. They computed 12 histograms, four for each color component from 12 DCT-VQ index sequences [9].

Texture is another salient and indispensable feature for CBIR. Smith et al. used the mean and variance of the wavelet coefficients as texture features for CBIR [10]. Birgale et al. [11] and Subrahmanyam et al. [12] combined the color (color histogram) and texture (wavelet transform) features for CBIR. Ahmadian et al. used the wavelet transform for texture classification [13]. Do et al. proposed the wavelet transform (DWT) based texture image retrieval using generalized Gaussian density and Kullback-Leibler distance (GGD &KLD) [14]. Unser used the wavelet frames for texture calsification and segmentation [15]. Manjunath et al. [16] proposed the Gabor transform (GT) for image retrieval on Bordatz texture database. They have used the mean and standard deviation features from four scales and six directions of Gabor transform. Kokare et al. used the rotated wavelet filters [17], dual tree complex wavelet filters (DT-CWF), dual tree rotated complex wavelet filters (DT-RCWF) [18],

rotational invariant complex wavelet filters [19] for texture image retrieval. They have calculated the characteristics of image in different directions using rotated complex wavelet filters.

B. Related Work

The recently proposed local binary pattern (LBP) features are designed for texture description. Ojala et al. proposed the LBP [20] and these LBPs are converted to rotational invariant for texture classification [21]. pietikainen et al. proposed the rotational invariant texture classification using feature distributions [22]. Ahonen et al. [23] and Zhao et al [24] used the LBP operator facial expression analysis and recognition. Heikkila et al. proposed the background modeling and detection by using LBP [25]. Huang et al. proposed the extended LBP for shape localization [26]. Heikkila et al. used the LBP for interest region description [27]. Li et al. used the combination of Gabor filter and LBP for texture segmentation [28]. Zhang et al. proposed the local derivative pattern for face recognition [29]. They have considered LBP as a nondirectional first order local pattern, which are the binary results of the first-order derivative in images. Subrahmanyam et al. [30] have proposed the directional binary wavelet patterns (DBWP) for biomedical image retrieval.

C. Main Contribution

To improve the retrieval performance in terms of retrieval accuracy, in this paper, we combined the color (HSV histogram) and texture (directional binary wavelet patterns) features. Two experiments have been carried out on Corel database and MIT VisTex databases for proving the worth of our algorithm. The results after being investigated show a significant improvement in terms of their evaluation measures as compared to HSV histogram and DBWP.

The organization of the paper as follows: In section I, a brief review of image retrieval and related work is given. Section II, III and IV, presents a concise review of HSV histogram, Local Binary Patterns and directional binary wavelet patterns (DBWP) respectively. Experimental results and discussions are given in section V. Based on above work conclusions are derived in section VI.

II. HSV COLOR HISTOGRAM

The color histogram is obtained by counting the number of times each color occurs in the image array. Histogram is invariant to translation and rotation of the image plane, and change only slowly under change of angle of view.

A color histogram H for a given image is defined as a vector

$$H = \{H[0], H[1], ..., H[i], ...H[N]\} \quad (1)$$

where i represent the color in color histogram and H[i] represent the number of pixels of HSV color i in the image, and N is the number of bins used in color histogram. For comparing the histogram of different sizes, color histogram should be normalized. The normalized color histogram is given as

$$H' = \frac{H}{p} \quad (2)$$

where p is the total number of pixels in the image.

In this paper, HSV color space is used i.e. histogram for each color channel is used as feature for image database.

III. LOCAL BINARY PATTERNS (LBP)

The LBP operator introduced by Ojala et al. [20] as shown in Fig. 1. For given a center pixel in the image, a LBP value is computed by comparing it with those of its neighborhoods:

$$LBP_{P,R} = \sum_{i=0}^{P-1} 2^i \times f(g_p - g_c) \quad (3)$$

$$f(x) = \begin{cases} 1 & x \geq 0 \\ 0 & x < 0 \end{cases} \quad (4)$$

where g_c is the gray value of the center pixel, g_i is the gray value of its neighbors, P is the number of neighbors and R is the radius of the neighborhood. Fig. 2 shows the examples of circular neighbor sets for different configurations of (P, R).

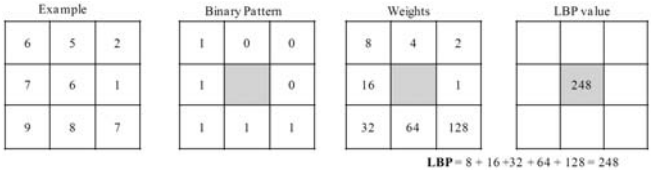

Fig. 1: LBP calculation for 3×3 pattern

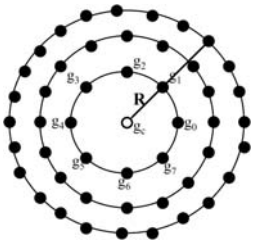

Fig. 2: Circular neighborhood sets for different *(P,R)*

IV. DIRECTIONAL BINARY WAVELET PATTERNS

Subrahmanyam et al. [30] have proposed the directional binary wavelet patterns (DBWP) for biomedical image retrieval. The brief description about DBWP is given in the following subsections.

A. 1-D Binary Wavelet Transform (1-D BWT)

The implementation of binary wavelet transform (BWT) on binary images is similar as the lifting wavelet transform is conducted on grayscale image.

Let x be an 1×N signal, the transformed BWT coefficients matrix T can be constructed as follows:

$$T = [C\ D]^T \tag{5}$$

where

$$C = (\bar{c}\,|_{s=0}, \bar{c}\,|_{s=2}, ..., \bar{c}\,|_{s=N-2})^T$$
$$D = (\bar{d}\,|_{s=0}, \bar{d}\,|_{s=2}, ..., \bar{d}\,|_{s=N-2})^T \tag{6}$$

$\bar{a}\,|_{s=k}$ defines a vector with elements formed from a circular shifted sequence of $\bar{a}$ by k. A^T is the transpose of A, and

$$\bar{c} = \{c_0, c_1, ...c_{S-1}\}^T$$
$$\bar{d} = \{d_0, d_1, ...d_{S-1}\}^T \tag{7}$$

S is the number of scales, c_i and d_i are the scaling (lowpass) and the wavelet coefficients (highpass) respectively. The BWT is then defined as:

$$y = T\ x \tag{8}$$

In [31], the 32 length-8 binary filters are classified into four groups depending on the number of "1"s in the binary filters. Examples of the binary filters in each group are given in Table 1.

B. In-place Implementation of BWT

Law and Siu [31] have proposed the implementation of BWT as similar to the lifting scheme in real wavelet transform by in-place implementation. In order to have an in-place implementation structure, the odd number and the even number samples of the original signal are split into two sequences. These two sequences are then updated according to the filter coefficients from the lowpass and the bandpass filters. This structure is similar to the ''split, update and predict'' procedure in the lifting implementation of the real field wavelet transform. The lowpass output and the bandpass output are interleaved together in the transformed output. BWT implementation with group 1 filter is conducted, where the all even number yields lowpass output, while odd number refers to bandpass output which are calculated by applying exclusive-or (XOR) operation between even and odd samples of input signal. The scheme is depicted in Fig. 3. Similar in-place structures can be extended easily to other groups.

TABLE 1: BINARY WAVELET FILTERS GROUPING OF LENGTH BEING EQUAL TO 8

Group	Lowpass filter	Highpass filter
1	{0, 1, 0, 0, 0, 0, 0 ,0}	{1, 1, 0, 0, 0, 0, 0 ,0}
2	{1, 1, 1, 0, 0, 0, 0 ,0}	{1, 1, 0, 0, 0, 0, 0 ,0}
3	{1, 1, 1, 1, 0, 0, 0 ,1}	{1, 1, 0, 0, 0, 0, 0 ,0}
4	{1, 1, 1, 1, 1, 1, 1 ,0}	{1, 1, 0, 0, 0, 0, 0 ,0}

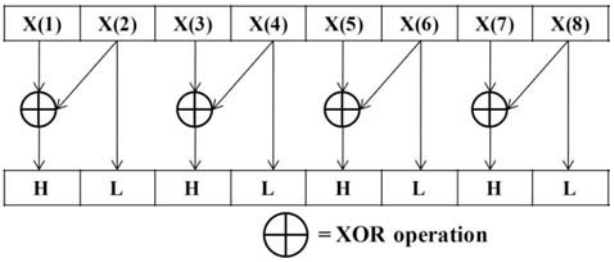

Fig. 3: In-place implementation of BWT for Group 1 filter

C. 2-D BWT

A separable 2-D binary wavelet transform can be computed efficiently in binary space by applying the associated 1-D filter bank to each row of the image, and then applying the filter bank to each column of the resultant coefficients.

In the first level of decomposition, one lowpass sub-image (LL) and three orientation selective highpass sub-images (LH, HL and HH) are created. In second level of decomposition, the lowpass sub-image is further decomposed into one lowpass (LL) and three highpass sub-images (LH, HL and HH). The process is repeated on the lowpass sub-image to form higher level of wavelet decomposition. In other words, BWT decomposes an image in to a pyramid structure of the sub-images with various resolutions corresponding to the different scales. Three-stage decomposition will create three lowpass sub-images and nine (three each in horizontal (0º), vertical (90º), and diagonal (45º) direction) highpass directional sub-images. The lowpass sub-images are low-resolution versions of the original image at different scales. The horizontal, vertical and diagonal sub-images provide the information about the brightness changes in the corresponding directions respectively.

Initially, the BWT is designed for image compression of binary images. Further, this concept has been extended on grayscale image by separating it into binary bit planes, and then performed the BWT to each individual bit plane of image.

D. Directional Binary Wavelet Patterns (DBWP)

The proposed DBWP encodes the directional edge information in a neighborhood with the help of BWT. Given an 8-bit grayscale image I, we separated it into 8 binary bit planes as follows:

$$I = \sum_{i=1}^{8} 2^{(i-1)} \times I^i \qquad (9)$$

where is the ith bit plane of image I.

The BWT is performed on each bit plane to extract the multi-resolution edge information in horizontal (00), vertical (900) and diagonal (±450) directions.

$$\left[W^i_{low,S+1}, W^i_{high(0^0),S+1}, W^i_{high(90^0),S+1}, W^i_{high(\pm 45^0),S+1}\right] = BWT(W^i_{low,S}); \quad i = 1,2,....8 \qquad (10)$$

$$W^i_{low,S} = \begin{cases} I^i & if\ S = 1 \\ W^i_{low,S} & else \end{cases} \qquad (11)$$

where the function [o]=BWT(x) denotes, the ouput ‘o’ for BWT operation of input ‘x’. S is the number of scales, W is the lowpass and highpass output in BWT operation.

Given a center pixel in the 3×3 pattern, DBWP value is computed by collecting its *P* neighborhoods based on Eq. (12).

$$DBWP^i_{P,R,S} = \sum_{p=1}^{P} 2^{(p-1)} \times W^i_S(g_p) \qquad (12)$$

where $W^i_S(g_p)$ denotes the binary value of its neighbors, *P* stands for the number of neighbors and *R*, the radius of the neighborhood.

After computing the DBWP pattern for each pixel in W^i_S, the whole subband is represented by a histogram using Eq. (13). Finally, these histograms (8×3×4) are calculated from three scales BWT on 8-bit planes and are concatenated to construct final feature vector.

The uniform DBWP/LBP pattern refers to the uniform appearance pattern which has limited discontinuities in the circular binary presentation. In this paper, the pattern which has less than or equal to two discontinuities in the circular binary presentation is considered as the uniform pattern and remaining patterns considered as non-uniform patterns.

Fig. 3 shows all uniform patters for *P=8*. The distinct values for given query image is $P(P-1)+3$ by using uniform patterns.

After identifying the LP (DBWP/LBP) pattern of each pixel *(j, k)*, the whole image is represented by building a histogram:

$$H_S(l) = \sum_{j=1}^{N_1} \sum_{k=1}^{N_2} f(LP^{u2}_{P,R}(j,k), l);\ l \in [0, P(P-1)+3] \qquad (13)$$

$$f(x,y) = \begin{cases} 1 & x = y \\ 0 & othrwise \end{cases} \qquad (14)$$

where the size of input image is $N_1 \times N_2$.

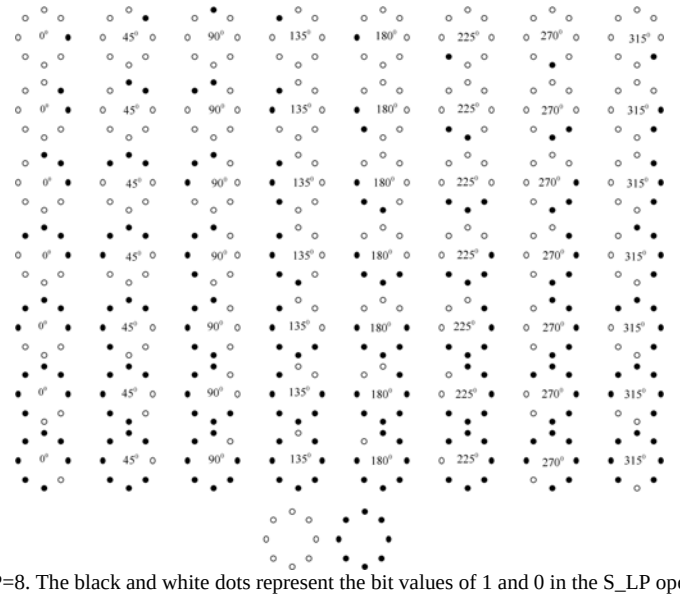

Fig. 4: Uniform patters when P=8. The black and white dots represent the bit values of 1 and 0 in the S_LP operator.

E. Proposed System Framework (CDBWP)

In this paper, we proposed the new technique by combining the color (HSV histogram) and texture (DBWP) for image retrieval. The algorithm for the proposed image retrieval system is given below:

Algorithm:
Input: Image; Output: Retrieval results.

1. Load the input image.
2. Covert the RGB image to HSV and gray images for color and texture features extraction respectively.
3. Construct the histogram on HSV spaces.
4. Collect the DBWP from gray image.
5. Construct the histograms of DBWP.
6. Form the feature vector by concatenating the both HSV and DBWP histograms.
7. Calculate the best matches using Eq. (17).
8. Retrieve the number of top matches.

F. Similarity Measurement

In the presented work *four* types of similarity distance metric ares used as shown below:

Manhattan or L_1 or city-block Distance

This distance function is computationally less expensive than Euclidean distance because only the absolute differences in each feature are considered. This distance is sometimes called the city block distance or L_1 distance and defined as

$$D(Q,T) = \sum_i \left| f_i(Q) - f_j(T) \right| \tag{15}$$

Euclidean or L_2 Distance

For p=2 in the equation (1.1) give the Euclidean distance and defined as:

$$D(Q,T) = \left(\sum_i \left| f_i(Q) - f_j(T) \right|^2 \right)^{1/2} \tag{16}$$

The most expensive operation is the computation of square root.

D_1 Distance

$$D(Q,T) = \sum_{i=1}^{Lg} \left| \frac{f_{T,i} - f_{Q,i}}{1 + f_{T,i} + f_{Q,i}} \right| \tag{17}$$

Canberra Distance

$$D(Q,T) = \sum_{i=1}^{Lg} \frac{\left| f_{T,i} - f_{Q,i} \right|}{\left| f_{T,i} + f_{Q,i} \right|} \tag{18}$$

where Q is query image, Lg is feature vector length, T is image in database; $f_{I,i}$ is i^{th} feature of image I in the database, $f_{Q,i}$ is i^{th} feature of query image Q.

Fig. 5: Sample images from Corel 1000 (one image per category)

V. EXPERIMENTAL RESULTS AND DISCUSSIONS

For the work reported in this paper, retrieval tests are conducted on two different databases (Corel 1000, and MIT VisTex) and results are presented separately.

A. Database DB1

Corel database [32] contains large amount of images of various contents ranging from animals and outdoor sports to natural images. These images are pre-classified into different categories of size 100 by domain professionals. Some researchers think that Corel database meets all the requirements to evaluate an image retrieval system, because of its large size and heterogeneous content. In this paper, we collected the database DB1 contains 1000 images of 10 different categories (groups *G*). Ten categories are provided in the database namely *Africans, beaches, buildings, buses, dinosaurs, elephants, flowers, horses, mountains and food*. Each category has 100 images ($N_G = 100$) and these have either 256×384 or 384×256 sizes. Fig. 5 depicts the sample images of Corel 1000 image database (one image from each category).

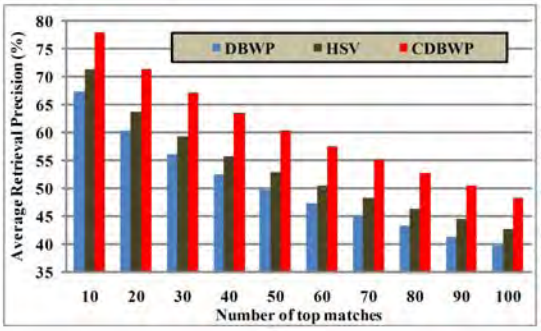

(a)

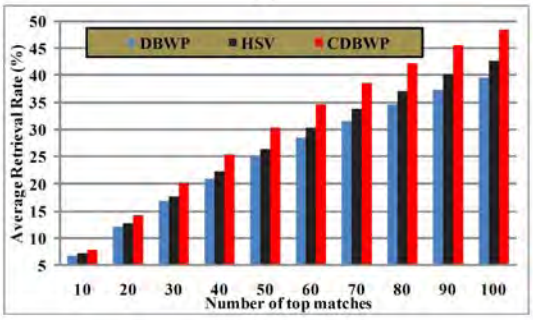

(b)

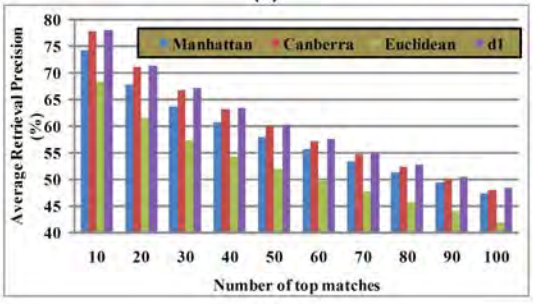

(c)

Fig. 6: Comparison of proposed method with various methods in terms of: (a) & (c) Average retrieval precision, (b) average retrieval rate according to no. of top matches considered

The performance of the proposed method is measured in terms of average precision and average recall by Eq. (19) and (20) respectively.

$$Precision\left[P(I_q,n)\right]=\frac{No.of\ \text{Re}levant\ Images\ Retrieved}{Total\ No.of\ Images\ Retrieved} \quad (19)$$

$$Recall\left[R(I_q,n)\right]=\frac{No.of\ Relevant\ Images\ Retrieved}{Total\ No.of\ Relevant\ Images\ in\ Database} \quad (20)$$

where I_q is the query image and n is number of top matches considered.

Table II and III summarizes the retrieval results of the proposed method (CDBWP) and other methods (HSV histogram and DBWP) in terms of average retrieval precision and recall respectively. From Table II and Table III, , it is clear that the proposed method showing better performance compared to HSV histogram and DBWP methods in terms of average retrieval precision and recall. Table IV and Fig. 6 (a) provides the comparison between various techniques in terms of average retrieval precision. From Table IV and Fig. 6 (a), it is clear that the proposed method (CDBWP) outperforms the HSV histogram and DBWP. Fig. 6 (b) illustrates the comparison between various methods in terms of average retrieval rate. Table V and Fig. 6 (c) provides the performance of proposed method using various distance measures. From Table V and fig. 6 (c), it is found that the d1 distance is outperforming the HSV histogram and DBWP.

TABLE II RESULTS OF ALL TECHNIQUES IN TERMS OF PRECISION ON DB1 DATABASE

Category	LBP	DBWP	HSV	CDBWP
Africans	61.8	69.7	75.5	82
Beaches	55.4	44.2	41.6	52
Buildings	65.4	56.4	65.1	72.9
Buses	96.7	87.6	87.3	94
Dinosaurs	98.4	98.2	100	99.5
Elephants	46.3	54.6	62	66.9
Flowers	92.2	91.4	77.5	95.2
Horses	76.7	74	93.9	93.9
Mountains	41.9	37.6	32	41.8
Food	68.6	58.8	78.4	81.5
Total	**70.3**	**67.25**	**71.33**	**77.97**

All evaluation values are in percentage (%)

TABLE III RESULTS OF ALL TECHNIQUES IN TERMS OF RECALL ON DB1 DATABASE

Category	LBP_8_1	DBWP	HSV	CDBWP
Africans	38.1	34.31	42.94	45.28
Beaches	35.4	25.66	19.4	27.23
Buildings	33.7	27.5	34.99	36.07
Buses	70.5	51.7	63.77	68.08
Dinosaurs	75.1	84.66	90.35	94.08
Elephants	25.4	24.94	29.01	29.81
Flowers	65.6	64.39	32.86	67.46
Horses	42.2	30.36	50.82	48.61
Mountains	26.9	22.28	14.55	20.37
Food	37.2	30.26	47.82	46.37
Total	**44.9**	**39.60**	**42.65**	**48.33**

All evaluation values are in percentage (%)

TABLE IV RESULTS OF VARIOUS TECHNIQUES IN TERMS OF AVERAGE RETRIEVAL PRECISION ON DB1 DATABASE

	10	20	30	40	50	60	70	80	90	100
DBWP	67.25	60.36	56.06	52.57	49.63	47.19	45.08	43.18	41.37	39.60
HSV	71.33	63.77	59.31	55.78	52.91	50.46	48.30	46.35	44.52	42.65
CDBWP	77.97	71.23	67.15	63.46	60.37	57.59	55.14	52.76	50.55	48.33

TABLE V RESULTS OF PROPOSED METHOD WITH DIFFERENT DISTANCE MEASURES IN TERMS OF AVERAGE RETRIEVAL RATE ON DB1 DATABASE

	10	20	30	40	50	60	70	80	90	100
Manhattan	74.3	67.74	63.62	60.69	57.98	55.66	53.37	51.32	49.32	47.35
Canberra	77.77	71.09	66.80	63.23	60.02	57.21	54.65	52.31	50.14	47.95
Euclidean	68.51	61.53	57.39	54.27	51.98	49.79	47.74	45.75	43.92	42.00
d1	77.97	71.23	67.15	63.46	60.37	57.59	55.14	52.76	50.55	48.33

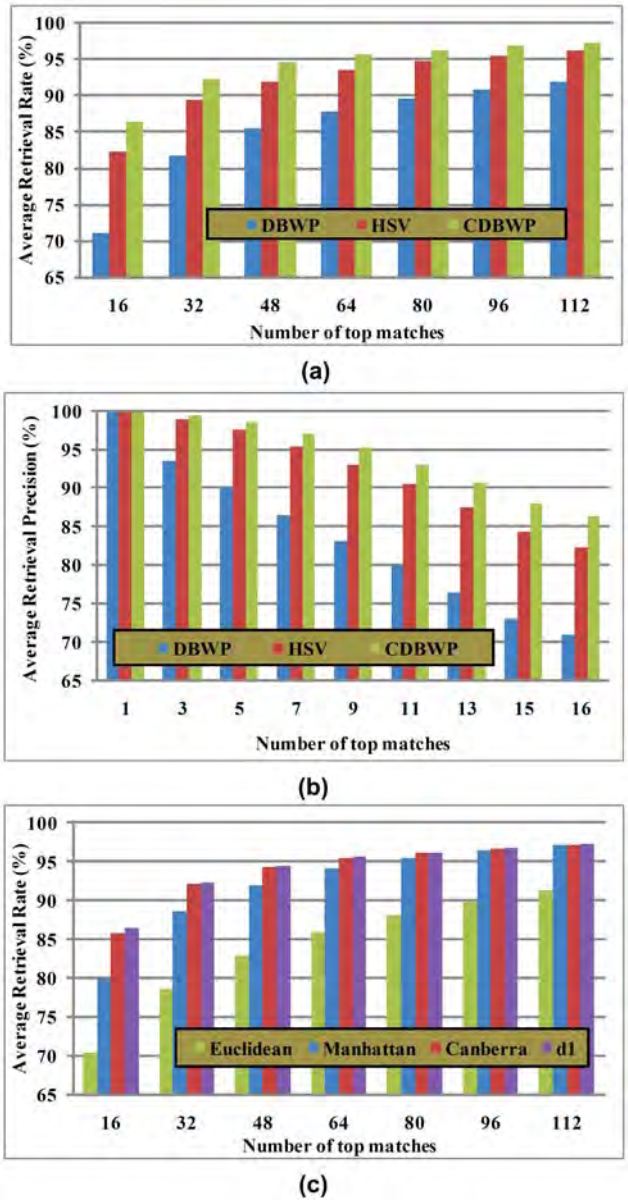

Fig. 7: Average retrieval precision of DB2 database according to no. of top matches considered

B. Database DB2

The database DB2 used in our experiment consists of 40 different textures [33]. The size of each texture is 512×512 . Each 512×512 image is divided into sixteen 128×128 non-overlapping sub-images, thus creating a database of 640 (40×16) images. The performance of the proposed method is measured in terms of average retrieval rate (ARR) is given by Eq. (21).

$$ARR = \frac{No.of\ Relevant\ Images\ Retrieved}{Total\ No.of\ Relevant\ Images\ in\ Database} \qquad (21)$$

The database DB2 is used to compare the performance of the proposed method (CDBWP) with HSV histogram and DBWP on texture database. Fig. 7 (a) and (b) illustrate the performance of various methods in terms average retrieval rate and average retrieval precision respectively. From Fig. 7 (a) and (b), it is clear that the proposed method showing better performance as compared to other methods. Fig. 7 (c) illustrates the performance of proposed method using various distance measures in terms of average retrieval rate. From Fig. 7 (c), it is clear that the d_1 distance showing better performance as compared to other distances.

VI. CONCLUSIONS

A new image indexing and retrieval algorithm is proposed in this paper by combining color (HSV histogram) and texture (DBWP) features for content based image retrieval. Two experiments have been carried out on Corel database and MIT VisTex for proving the worth of our algorithm. The results after being investigated shows a significant improvement in terms of their evaluation measures as compared to HSV histogram and DBWP techniques.

REFERENCES

[1] Y. Rui and T. S. Huang, Image retrieval: Current techniques, promising directions and open issues, J.. Vis. Commun. Image Represent., 10 (1999) 39–62.

[2] A. W.M. Smeulders, M. Worring, S. Santini, A. Gupta, and R. Jain, Content-based image retrieval at the end of the early years, IEEE Trans. Pattern Anal. Mach. Intell., 22 (12) 1349–1380, 2000.

[3] M. Kokare, B. N. Chatterji, P. K. Biswas, A survey on current content based image retrieval methods, IETE J. Res., 48 (3&4) 261–271, 2002.

[4] Ying Liu, Dengsheng Zhang, Guojun Lu, Wei-Ying Ma, Asurvey of content-based image retrieval with high-level semantics, Elsevier J. Pattern Recognition, 40, 262-282, 2007.

[5] M. J. Swain and D. H. Ballar, Indexing via color histograms, Proc. 3rd Int. Conf. Computer Vision, Rochester Univ., NY, (1991) 11–32.

[6] M. Stricker and M. Oreng, Similarity of color images, Proc. SPIE, Storage and Retrieval for Image and Video Databases, (1995) 381–392.

[7] G. Pass, R. Zabih, and J. Miller, Comparing images using color coherence vectors, Proc. 4th ACM Multimedia Conf., Boston, Massachusetts, US, (1997) 65–73.

[8] J. Huang, S. R. Kumar, and M. Mitra, Combining supervised learning with color correlograms for content-based image retrieval, Proc. 5th ACM Multimedia Conf., (1997) 325–334.

[9] Z. M. Lu and H. Burkhardt, Colour image retrieval based on DCT domain vector quantization index histograms, J. Electron. Lett., 41 (17) (2005) 29–30.

[10] J. R. Smith and S. F. Chang, Automated binary texture feature sets for image retrieval, Proc. IEEE Int. Conf. Acoustics, Speech and Signal Processing, Columbia Univ., New York, (1996) 2239–2242.

[11] L. Birgale, M. Kokare, D. Doye, Color and Texture Features for Content Based Image Retrieval, International Conf. Computer Grafics, Image and Visualisation, Washington, DC, USA, (2006) 146 – 149.

[12] Subrahmanyam, A. B. Gonde and R. P. Maheshwari, Color and Texture Features for Image Indexing and Retrieval, IEEE Int. Advance Computing Conf., Patial, India, (2009) 1411-1416.

[13] A. Ahmadian, A. Mostafa, An Efficient Texture Classification Algorithm using Gabor wavelet, 25th Annual international conf. of the IEEE EMBS, Cancun, Mexico, (2003) 930-933.M.

[14] M. N. Do and M. Vetterli, "The contourlet transform: An efficient directional multi-resolution image representation," IEEE Trans. Image Process., vol. 14, no. 12, pp. 2091–2106, 2005.

[15] M. Unser, Texture classification by wavelet packet signatures, IEEE Trans. Pattern Anal. Mach. Intell., 15 (11): 1186-1191, 1993.

[16] B. S. Manjunath and W. Y. Ma, Texture Features for Browsing and Retrieval of Image Data, IEEE Trans. Pattern Anal. Mach. Intell., 18 (8): 837-842, 1996.

[17] M. Kokare, P. K. Biswas, B. N. Chatterji, Texture image retrieval using rotated Wavelet Filters, Elsevier J. Pattern recognition letters, 28:. 1240-1249, 2007.
M. Kokare, P. K. Biswas, B. N. Chatterji, Texture Image Retrieval Using New Rotated Complex Wavelet Filters, IEEE Trans. Systems, Man, and Cybernetics, 33 (6): 1168-1178, 2005.

[18] M. Kokare, P. K. Biswas, B. N. Chatterji, Rotation-Invariant Texture Image Retrieval Using Rotated Complex Wavelet Filters, IEEE Trans. Systems, Man, and Cybernetics, 36 (6): 1273-1282, 2006.

[19] T. Ojala, M. Pietikainen, D. Harwood, A comparative sudy of texture measures with classification based on feature distributions, Elsevier J. Pattern Recognition, 29 (1): 51-59, 1996.

[20] T. Ojala, M. Pietikainen, T. Maenpaa, Multiresolution gray-scale and rotation invariant texture classification with local binary patterns, IEEE Trans. Pattern Anal. Mach. Intell., 24 (7): 971-987, 2002.

[21] M. Pietikainen, T. Ojala, T. Scruggs, K. W. Bowyer, C. Jin, K. Hoffman, J. Marques, M. Jacsik, W. Worek, Overview of the face recognition using feature distributions, Elsevier J. Pattern Recognition, 33 (1): 43-52, 2000.

[22] T. Ahonen, A. Hadid, M. Pietikainen, Face description with local binary patterns: Applications to face recognition, IEEE Trans. Pattern Anal. Mach. Intell., 28 (12): 2037-2041, 2006.

[23] G. Zhao, M. Pietikainen, Dynamic texture recognition using local binary patterns with an application to facial expressions, IEEE Trans. Pattern Anal. Mach. Intell., 29 (6): 915-928, 2007.

[24] M. Heikkil;a, M. Pietikainen, A texture based method for modeling the background and detecting moving objects, IEEE Trans. Pattern Anal. Mach. Intell., 28 (4): 657-662, 2006.

[25] X. Huang, S. Z. Li, Y. Wang, Shape localization based on statistical method using extended local binary patterns, Proc. Inter. Conf. Image and Graphics, 184-187, 2004.

[26] M. Heikkila, M. Pietikainen, C. Schmid, Description of interest regions with local binary patterns, Elsevie J. Pattern recognition, 42: 425-436, 2009.

[27] M. Li, R. C. Staunton, Optimum Gabor filter design and local binary patterns for texture segmentation, Elsevie J. Pattern recognition, 29: 664-672, 2008.

[28] B. Zhang, Y. Gao, S. Zhao, J. Liu, Local derivative pattern versus local binary pattern: Face recognition with higher-order local pattern descriptor, IEEE Trans. Image Proc., 19 (2): 533-544, 2010.

[29] Subrahmanyam Murala, Maheshwari R.P., Balasubramanian R., Directional binary wavelet patterns for biomedical image indexing and retrieval, Proc. J. Med. Syst. doi:10.1007/s10916-011-9764-4.

[30] N.F. Law, and W.C. Siu, A filter design strategy for binary field wavelet transform using the perpendicular constraint, J. Signal Process. 87 (11) 2850–2858, 2007.

[31] Corel 1000 and Corel 10000 image database. [Online]. Available: http://wang.ist.psu.edu/docs/related.shtml.

[32] MIT Vision and Modeling Group, Vision Texture. [Online]. Available: http://vismod.www.media.mit.edu.

Dr.A.Rama Mohan Reddy working as Professor & HOD of Computer Science and Engineering, Sri Venkateswara University, Tirupati,A.P.,INDIA. He Completed M.Tech (Computer Science) from NIT, Warangal. He completed his Ph.D. in the area of software Architecture. He has more than 20 years of teaching experience. He published many papers in the peer-refereed journals and conferences. His interested areas are Software Engineering and Software Architecture, Data Mining.

P.Vijaya Bhaskar Reddy is a Research Scholar in Computer science and Engineerin Department Sri Venkateswara University, Tirupati,A.P.,INDIA. He Completed M.Tech (Computer Science) from Bharath University, Chennai